crystals

MDPI

Article

Nematic Phase Induced from Symmetrical Supramolecular H-Bonded Systems Based on Flexible Acid Core

Hoda A. Ahmed [1,2,*] and Muna S. Khushaim [3,4]

1 Faculty of Science, Department of Chemistry, Cairo University, Cairo 12613, Egypt
2 Chemistry Department, College of Sciences, Taibah University, Yanbu 30799, Saudi Arabia
3 Department of Physics, Faculty of Science, Taibah University, Al-Madina 41447, Saudi Arabia; mkhushaim@taibahu.edu.sa
4 Nanotechonolgy Center, Taibah University, Al-Madina 41447, Saudi Arabia
* Correspondence: ahoda@sci.cu.edu.eg

Received: 9 August 2020; Accepted: 8 September 2020; Published: 10 September 2020

Abstract: New symmetrical 1:2 supramolecular H-bonded liquid crystals (SMHBLCs) interactions, **A/2Bn**, were formed between adipic acid and 4-(4′–pyridylazophenyl) 4″-alkoxybenzoates. Optical and mesomorphic behaviors of the prepared SMHBLC complexes were investigated using differential scanning calorimetry (DSC), polarizing optical microscopy (POM) and X-ray diffraction (XRD). FT-IR spectroscopy was carried out to confirm the H-bond interactions of the prepared complexes via Fermi bands formation. Their photo-physical properties were investigated by UV-spectroscopy and the observed absorbance values were found to be mainly dependent on the length of the terminal alkoxy chain. Mesomorphic behaviour for all **A/2Bn** complexes revealed that all complexes are dimorphic-exhibiting enantiotropic mesophases with induced nematic phases, except for the long chain terminal complex which exhibits only a monomorphic smectic A phase. In order to investigate the effect of mesogenic core geometry on the mesophase properties, a comparison was established between the mesomeric behaviors of the present complexes and previously reported rigid core acid complexes. Finally, the XRD pattern confirmed the POM and DSC results.

Keywords: adipic acid; supramolecular H-bonding complexes; X-ray diffraction; induced nematic phase; photo-physical properties

1. Introduction

In the last few years, liquid crystal (LC) technologies induced great effects in different engineering display applications [1–4]. Interesting studies have synthesized and designed enormous new mesogenic structures for display applications [5–10]. The formation of photosensitive supramolecular hydrogen-bonded liquid crystals (SMHBLCs) through intermolecular hydrogen bonding (H-bonding) interactions occupies a wide area of interests [11–19]. Various types of SMHBLCs, as single-bonded [20,21], double-bonded [22,23] and multiple-bonded [24,25] complexes have been investigated and reported.

The molecular architecture and the length of the terminal flexible chain of the liquid crystalline molecule play a significant role in the formation, type, thermal stability and temperature range of the mesophase. In such cases, as the terminal chain length increases, the molecules will be oriented in a parallel arrangement [26]. In addition, the terminal chain length has an important role in influencing

the twist-bend and heliconical nematic phases [27,28]. Furthermore, H-bonding interactions play a key role in the association of the molecules. H-bonding leads to an increase in mesogenic core moiety length, resulting in the inducement of mesophases to the formed complex.

Azo-pyridine-based LCs moieties have recently been synthesized, and their mesomorphic behaviour investigated [5,29,30]. The addition of azo-pyridine influences the powerful polar induction [31] and enhances the conjugation power of the mesogenic core, which offers a photonic application [32]. Moreover, the trans-cis-isomerization ability of azo-pyridines, upon thermal and photo irradiation, makes them suitable and interesting candidates for the study of photo-responsive properties [33–37]. Our choice of azopyridine derivatives was not only to introduce the azobenzene groups in the same complex as the flexible acid derivative, but also because of, firstly, their known abilities to induce liquid crystalline phases upon mixing with nonmesomorphic materials [38,39] and, secondly, they are also able to modify to a great extent the phase behaviour of liquid crystalline materials upon mixing with mesomorphic materials [40].

Combining rigid (aromatic rings) and flexible ((CH_2)n) components are essential in the formation of the anisotropic LCs complexes with better phase behaviour. From this point of view, the aim of our study is the construction of new geometrical symmetrical 1:2 supramolecular H-bonded complexes based on the reaction between adipic acid (**A**), as flexible core, and azopyridine base moeity (**Bn**) [29,40], with different terminal alkoxy chain lengths (n). This study evaluates their ability for H-bonding formation with molar ratio 1:2 (**A:2Bn**, Scheme 1) and investigates their mesomorphic and optical behaviour, as well as their photo-physical properties. Moreover, is to investigate how the mesomorphic and optical properties are impacted by the terminal length of the base component. Furthermore, a comparison is established between the present flexible core series and previously rigid cores SMHB complexes [40] to investigate the effect of the exchange of the mesogenic core, of the acid moiety, on mesophase characters.

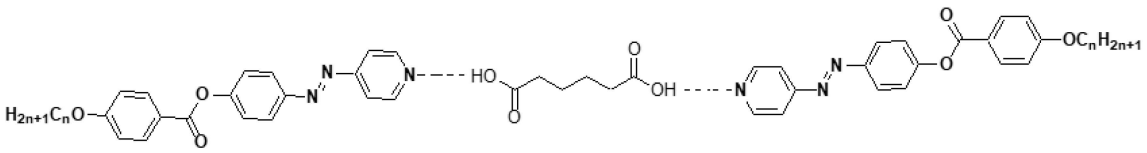

A/2Bn

Scheme 1. 1:2 supramolecular H-bonded liquid crystal (SMHBLC) complexes **A/2Bn**.

2. Experimental

The azo-pyridine base derivatives **Bn** were synthesized according to the previous procedure [29,40], which is attached in the Supplementary Materials.

Preparation of 1:2 SMHBLC Complexes

A/2Bn supramolecular complexes were formed from one mole of adipic acid (**A**) and two moles of azo-pyridine base (**Bn**) bearing different terminal alkoxy chain lengths that varied between n = 8 to n = 14. The solid mixture was melted with stirring to form an intimate blend and then allowed to cool to room temperature (Scheme 2). The formation of the supramolecular complexes (**A/2Bn**), were confirmed via DSC and FT-IR spectroscopy.

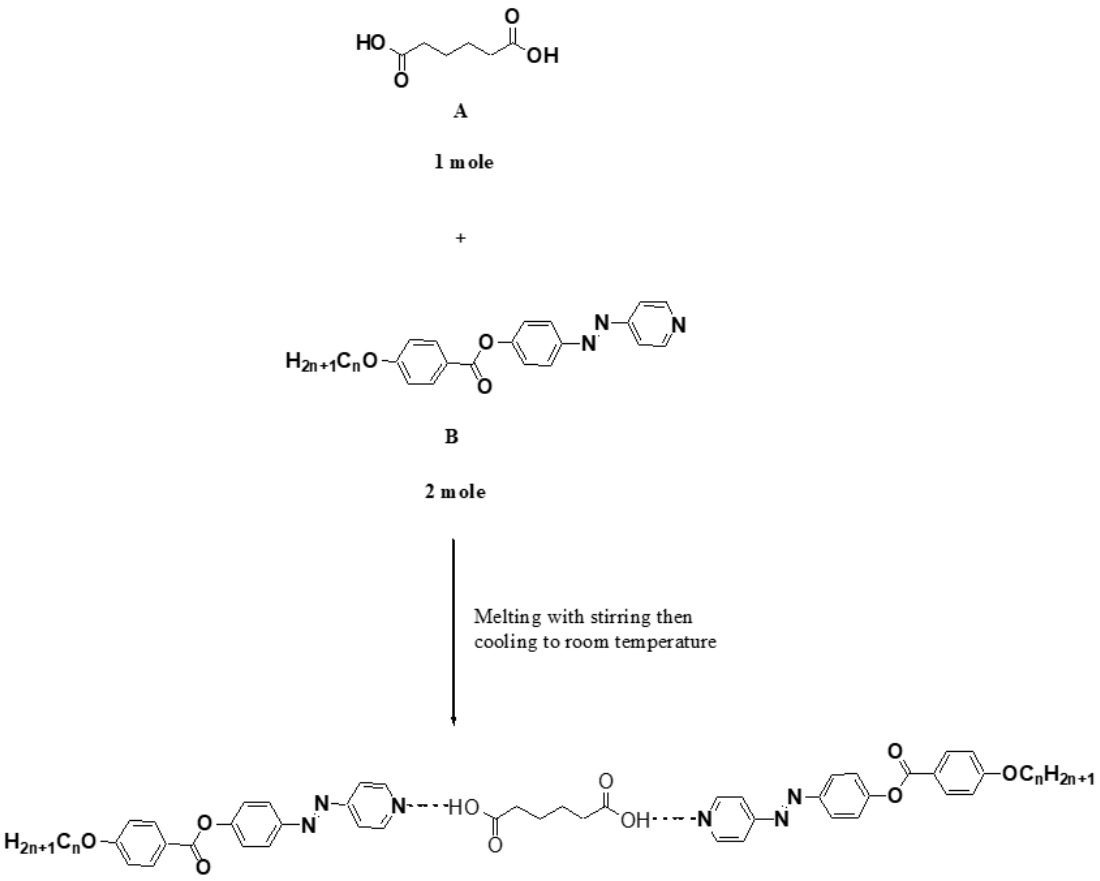

Scheme 2. Preparation of 1:2 SMHBLC complexes (**A/2Bn**).

3. Results and Discussion

3.1. FT-IR Characterizations of 1:2 SMHBLC Complexes

SMHBLC complex formation via H-bonding interactions of azo-pyridine (**Bn**) and adipic acid (A) with molar ratio 2:1 was confirmed by FT-IR spectral data. FT-IR measurements were performed for the two individual components as well as their 1:2 SMHBLC mixtures. FT-IR spectra of A, B10 and their complex **A/2B10** are given in Figure 1 as representative examples. The signal at 1649 cm^{-1} is assigned to the C=O group of the adipic acid (A). The important evidence of the H-bonded interactions formation is the C=O, OH stretching vibration. It has been reported [41–48] that the presence of three Fermi-resonance vibration bands (A-, B- and C-types) of the H-bonded OH groups is a confirmation of the SMHB formation. The A-type Fermi-band of the complex **A/2B10** is overlapped with that of the C-H vibrational peaks at 2922 to 2853 cm^{-1}. Furthermore, the observed peak at 2354 cm^{-1} for (**A/2B10**) could be assigned to the B-type of the in-plane bending vibration of the OH group. On the other hand, the band at 1920 cm^{-1} that corresponds to C-type Fermi-band is attributed to the molecular interactions between the overtone of the fundamental stretching vibration of the OH group and the torsional effect.

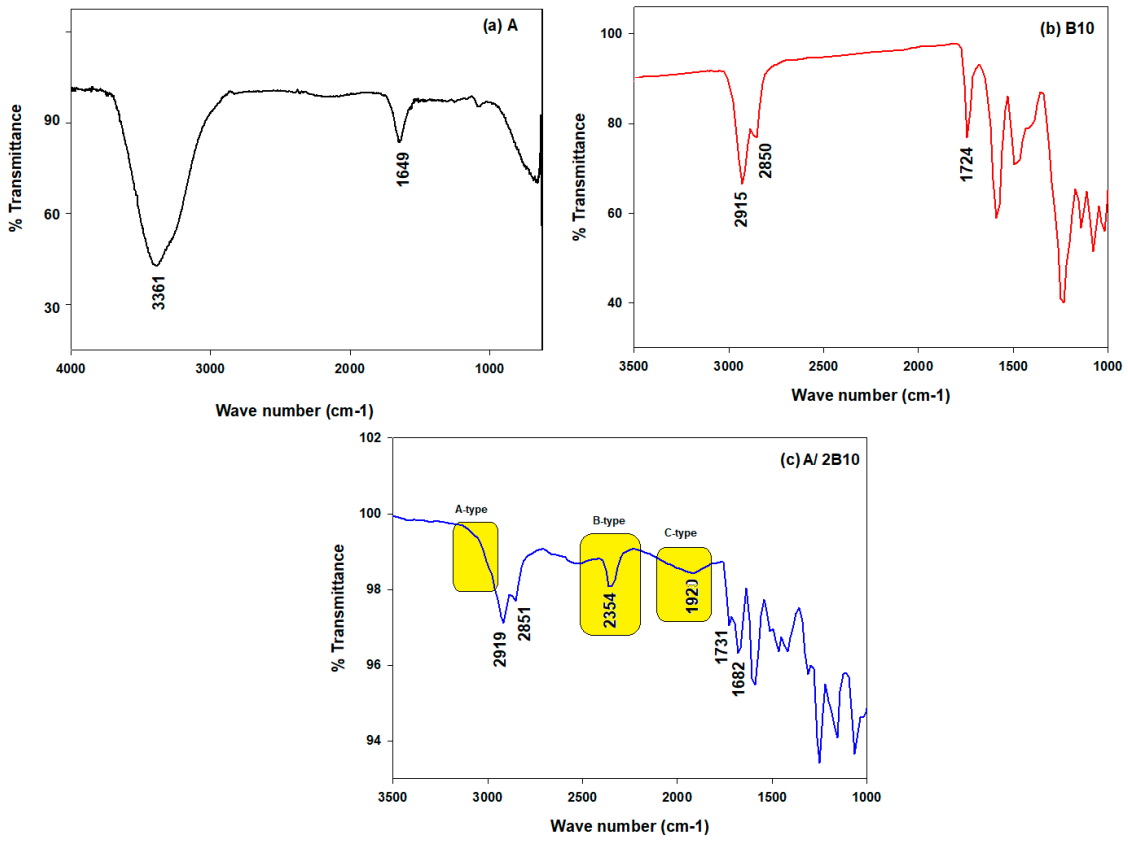

Figure 1. FT-IR spectra of (**a**) **A**; (**b**) **B10** and (**c**) **A/2B10**.

3.2. Mesophase Behavior of 1:2 SMHBLC Complexes, A/2Bn

Mesomorphic and optical behaviors for the present symmetrical 1:2 SMHBCs (**A/2Bn**) were investigated by DSC and POM. The results determined by DSC, given as phase transition temperatures (*T*), associated enthalpy (Δ*H*) and their normalized entropy (Δ*S*/*R*), for all prepared mixtures (**A/2Bn**), are summarized in Table 1. Representative examples of DSC curves taken from the second heating/cooling scans are represented in Figure 2. Textures of mesophases and optical behaviour of the present 1:2 SMHBCs were also investigated by POM. Moreover, POM observation textures are depicted in Figure 3. In order to ensure the stability of the prepared complexes, the DSC measurements were performed for two heating–cooling cycles and found to be the same. All thermal analyses were recorded from the second heating scan for all complexes. DSC measurements were confirmed by the POM texture observations. Transition temperature dependences on the terminal chain-length were graphically represented for the characterized complexes, **A/2Bn** (Figure 4). Figure 4 was constructed in order to investigate the effect of the terminal flexible chain lengths of the base components on the mesomorphic behaviour.

Table 1. Phase transition temperatures (*T*, °C), enthalpy of transitions (Δ*H*, kJ/mol) and normalized transition entropy (Δ*S*) of supramolecular complexes **A/2Bn**.

System	$T_{Cr\text{-}SmA}$	$\Delta H_{Cr\text{-}SmA}$	$T_{SmA\text{-}I}$	$\Delta H_{SmA\text{-}I}$	$T_{SmA\text{-}N}$	$\Delta H_{SmA\text{-}N}$	$T_{N\text{-}I}$	$\Delta H_{N\text{-}I}$	$\Delta S_{SmA}/R$	$\Delta S_N/R$
A/2B8	139.5	76.07	-	-	159.1	7.80	171.2	3.86	2.17	1.04
A/2B10	131.0	78.90	-	-	156.8	6.41	166.1	3.76	1.79	1.03
A/2B12	130.3	77.58	-	-	149.7	4.98	161.7	3.49	1.42	0.97
A/2B14	126.5	70.61	138.4	4.48	-	-	-	-	1.31	-

Abbreviations: Cr-SmA = Solid to smectic A transition; SmA-I = Smectic A to isotropic liquid transition; SmA-N = Smectic A to nematic transition; N-I = Nematic to isotropic liquid transition.

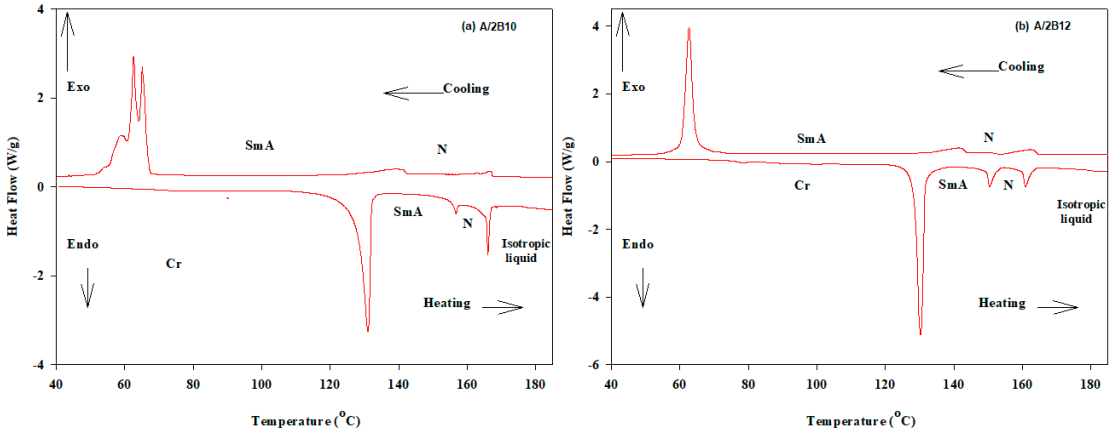

Figure 2. Differential scanning calorimetry (DSC) thermograms upon the second heating/cooling cycles at rate 10 °C/min for 1:2 SMHBLC complexes (**a**) **A/2B10** and (**b**) **A/2B12**.

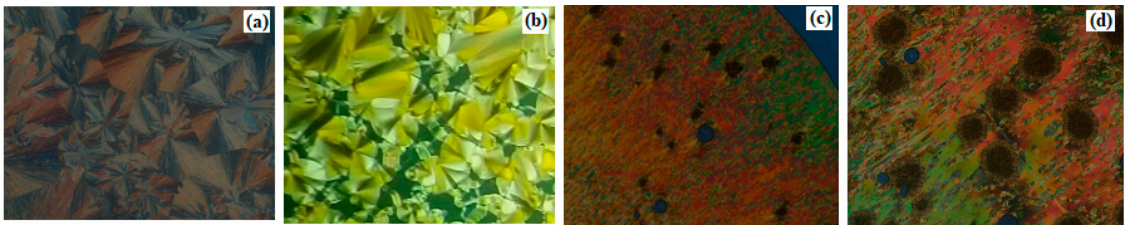

Figure 3. Mesophases textures under polarizing optical microscopy (POM) upon heating of **A/2B10** SMHBLC complex (**a**) Solid phase at 100.0 °C; (**b**) SmA phase at 141.0 °C; (**c**) N phase at 158.0 °C and (**d**) N and isotropic phases at 160.0 °C.

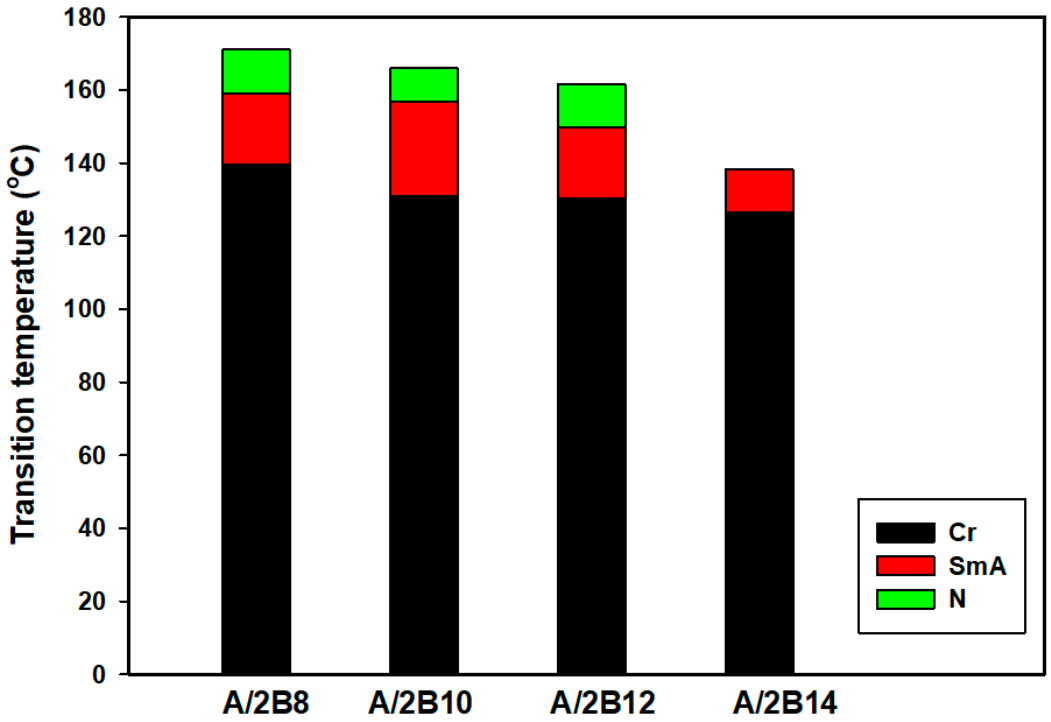

Figure 4. DSC graphical transitions of 1:2 SMHBLC complexes series, **A/2Bn**.

It should be mentioned here that the adipic acid spacer (**A**) is non-mesomorphic (converted from solid to liquid state directly upon heating), whereas the azo-pyridine derivatives (**Bn**) are smectogenic, exhibiting the smectic A (SmA) phase, except for the homologue **B8** which have dimorphic mesophases (SmA and N phases, see Table S2 in supplementary materials) [29,40]. Therefore, it was interesting to investigate the mesophase properties of the complexes resulting from mixing derivatives A and Bn.

The characteristic textures under POM (Figure 3) have solid phases that converted to smetic A and were followed by N mesophase observations for the prepared SMHBCs **A/2B8**, **A/2B10** and **A/2B12**. Meanwhile, the **A/2B14** homologue only transitions from the solid phase to SmA then to the isotropic liquid phase upon heating, and returns on cooling.

As can be seen from Table 1 and Figure 4, all the formed SMHBCs are enantiotropic and mesomorphic, exhibiting high thermal stabilities with an induced nematic phase. Moreover, the results revealed that the 1:2 complexes possess irregular melting temperatures with respect to the terminal chains (n). It can also be seen from Figure 4, that the nematic phase stability decreases, as usual, with the chain length of terminal base and vanishes at n = 14. In general, the terminal chain length and the mesogenic core of the H-bonded complexes play important roles in impacting the stability of the formed mesophase. In addition, it was found that the difference in polarity between H-donors and H-acceptors affects the H-bonding strength and influences the molecular anisotropy then promotes broadening of the mesomorphic range [49]. However, the length of the terminal alkoxy chain of the mixture does not affect the polarity of either component.

In the case of the **A/2B8** complex, the investigated data revealed that it is dimorphic, exhibiting the smectic A phase followed by an induced nematic phase, with a relatively broad temperature range (~12.1 °C). The smectic and nematic phase stabilities are 159.1 and 171.2 °C, respectively. Thus, the H-bonding interactions that enhance the stability of the SmA and lead to the formation of the induced N phase are found to be effective. Also for the homologues **A/2B10** and **A/2B12** complexes, the 1:2 mixtures are dimorphic, possessing SmA and N mesophases with thermal stabilities 156.8, 166.1, 149.7 and 161.7 °C, respectively. Thus, the increment of the molecular anisotropy will impact the nematic phases range, agreeing with previously reported work [49] which states that the increment of the mesogenic core length enhances the nematic phase stability.

In the case of the **A/2B14** mixture, only the SmA phase has been observed with mesophase stability 138.4 °C and smectogenic range ~11.9 °C. The vanishing of the N phase at terminal chain length n = 14 can be attributed to the rigid mesogenic core dilution [28]. Additionally, the higher attractions of Van der Waals between longer alkoxy chains increases the terminal interaction and alkyl group aggregation, which affects the formed mesophase.

It is well known that the mesophase behaviour of a certain liquid crystalline molecule depends mainly on its mesomeric properties, namely, inter molecular interactions and the molecular shape. In the present SMHBCs, **A/2Bn**, the mesophase stability depends mainly on several factors:

1. Lateral adhesion of molecules which increases with the increase of the base alkoxy-chain length or aspect ratio. In addition, the alkoxy chain length seems to play a significant role in the stabilization of mesophases of the SMHBCs.
2. Molecular geometry which is actually a function of the structure of the complexes, which in many cases is affected by the steric hindrance of the attached groups.
3. End-to-end interaction which depends mainly on the polarity and the length of the terminal substituents that result in the variation of the polarizability.

On the other side, the linking groups greatly affect the conjugation within the mesogenic core of the molecule.

3.3. Entropy Changes

As driven from DSC measurements, the normalized transition entropies ($\Delta S/R$) were estimated for the present symmetric 1:2 SMHBCs (**A/Bn**) and collected in Table 1. The graphical dependence of the entropy change on the alkoxy chain length of the azo-pyridine derivatives is depicted in Figure 5. As can be seen from Table 1 and Figure 5, the decrement of the entropy change ($\Delta S/R$) with the terminal alkoxy chain length (n) have been observed for both smectic and nematic transitions. In addition, the entropy changes of N-isotropic transitions, $\Delta S_N/R$, possess lower values compared to their corresponding smectic A transition entropy changes, $\Delta S_{SmA}/R$; this is in agreement with the previous reports [28]. It can be concluded that the decrement of the entropy changes with the increase in the terminal alkoxy-chain lengths is due to the increase in the biaxiality of the mesogenic part, which results in decreasing the conformational entropy. Moreover, this may be further attributed to the change in geometrical interactions between individual components of the complex, which is accordingly affected by the polarizability and the molecular shape of the molecule.

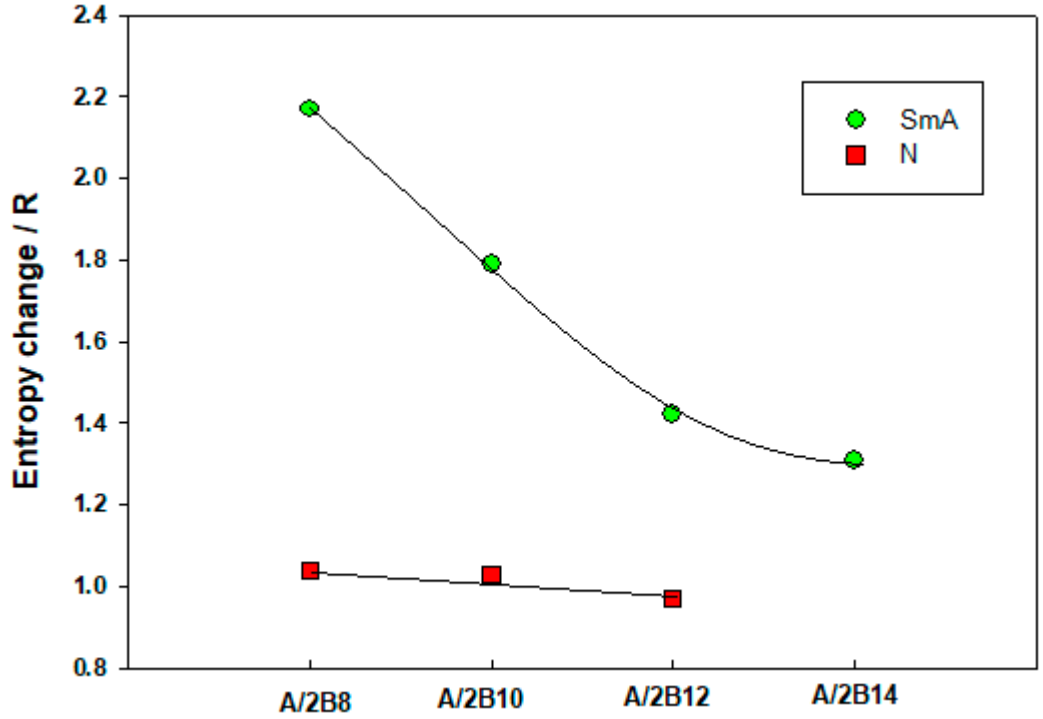

Figure 5. Entropy changes with the alkoxy chain length (n) of present SMHBLC complexes **A/2Bn**.

3.4. Effect of Changes in the Mesogenic Cores

In order to investigate the effect of an exchange in the mesogenic core of the flexible acid component on the mesomorphic properties, a comparison was made between the mesophase behaviour of present investigated five rings SMHBCs **A/2Bn**, with a flexible acid spacer core, and the previously reported 1:1 complexes **Cm/Bn**, possessing the rigid core acid moieties (4-alkoxy benzoic acid) [40] (Figure 6). The comparison indicated that the addition of a flexible chain core in the molecular geometry destabilizes the mesomorphic stability and induces new nematic transitions in most of the complexes. Meanwhile, all reported SMHBLC complexes **Cm/Bn** [40] exhibit high transition stabilities for the SmA and SmC mesophases. The stability increments of alkoxy benzoic acid complexes (Figure 6) are attributed to the increase in polarizability of their molecules, as well as their rigidity, which leads to the increase in the intermolecular interactions between individual molecules.

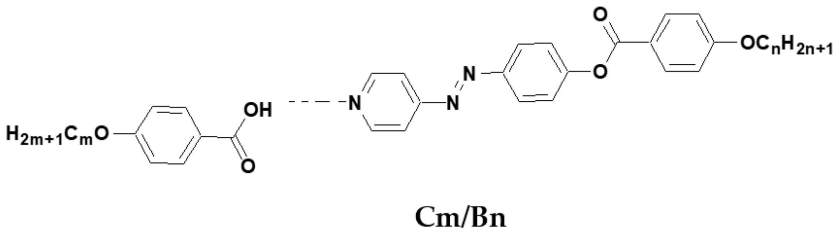

Cm/Bn

Figure 6. SMHBLC complexes of 1:1 **Cm/Bn**.

3.5. Photo-Physical Study

The photo-physical investigation of the present 1:2 SMHBCs **A/2Bn** was carried out by measuring UV-vis spectra. A solution of C = 1.8 × 10^{-6} mol/L in chloroform was used to estimate the spectro-photometric absorption spectra. Azopyridines undergoes cis/trans isomerization when irradiated with light of an appropriate wavelength. Those phenomena make it a suitable component of various molecular devices as well as functional materials [50,51]. Figure 7 shows the effects of UV irradiation on the UV-vis spectra of the base derivatives (**Bn**) in chloroform solution. It can be seen from Figure 7 that the light radiation in the wavelength range 290–500 nm is found to be strongly absorbed with the maximum at 349–350 nm, with another small peak at 456 nm for all derivatives with trans-conformation, which can be attributed to the π–π* transition of the chromophore in the molecule. [50,51] The resulting absorption bands of the present complexes (**A/2Bn**) are graphically represented in Figure 8. As shown from Figure 8, the formed 1:2 SMHBCs **A/2Bn** possess maximum absorption bands within ~450–454 nm according to the terminal alkoxy chain length of the base component (n). The highly delocalized electronic systems and π–π* transitions were attributed to the maximum absorption in the present H-bonding interactions for **A/2B12** complex. Moreover, the absorption and intensity of the peak in the absorption spectrum depend on the structure of the molecule that absorbs the light at a given wavelength. The change occurred in the UV-vis spectra of the base homologues (**Bn**), confirming the complexation. The complex **A/2B12** absorption spectra (Figure 8) showed the maxima bands at 454 nm, which is attributed to the electronic transition from the highest occupied molecular orbitals (HOMO) to lowest unoccupied molecular orbital (LUMO), π–π transition [47–49,52–54].

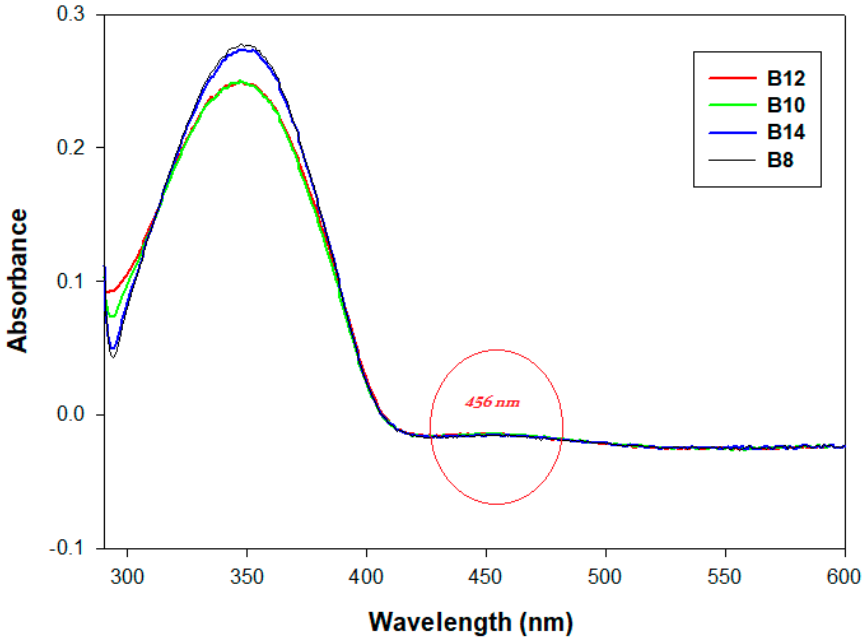

Figure 7. UV absorption spectrum of **Bn** derivatives in chloroform.

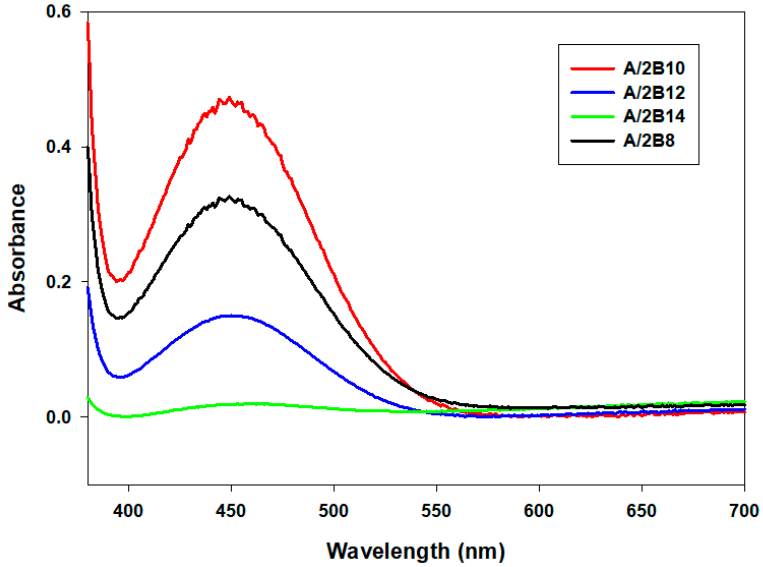

Figure 8. UV absorption spectrum of 1:2 SMHBCs, **A/2Bn**, in chloroform.

3.6. X-ray Diffraction Investigation

Another tool to confirm the mesophase assignments (SmA and N phases), X-ray diffraction investigation at different temperatures upon cooling from the isotropic liquid phase, was performed for the homologue **A/2B10** as an example for the present 1:2 SMHBCs complexes series (Figure 9). As can be seen from Figure 8, XRD analysis patterns showed a broad peak at angle 2θ = 23.5° indicating the presence of a nematic transition phase upon cooling for both recorded temperatures which related to the lateral interactions between mesogenic groups. Another small peak in high angle value was observed (2θ = 50.0°) corresponding to the SmA transitions. The formation of the smectic phase is proved by the existence of the X-ray small-angle reflection corresponding to the layer distance. Generally, the wide-peak angles reflect to lateral interactions of the N phases [55]. Temperature-dependent XRD measurements of the prepared complexes confirmed the presence of the SmA and N phases. The XRD pattern was consistent with the intrinsic character of each mesophase. By combining the XRD results and POM investigations, the existence of both the smectic A and N mesophases in the formed SMHBCs **A/2Bn** series was confirmed.

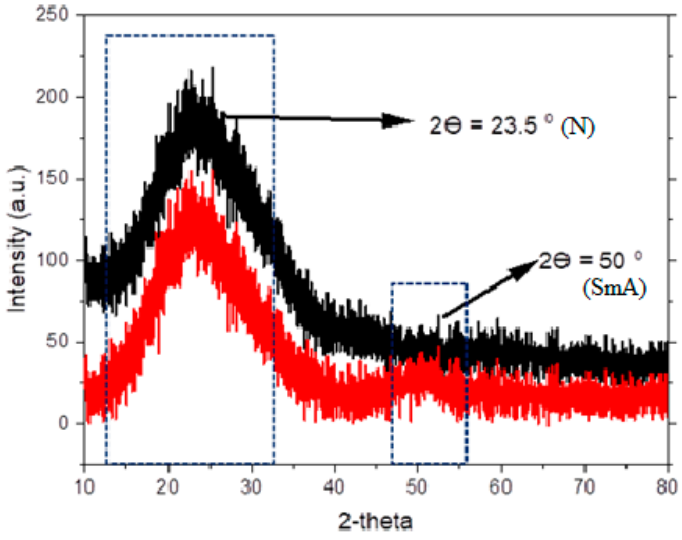

Figure 9. X-ray diffraction patterns of **A/2B10** at different temperatures upon cooling from the isotropic liquid phase.

4. Conclusions

A new series of 1:2 SMHBLC complexes, bearing symmetric alkoxy group terminals with different lengths was prepared, and investigated by different techniques. The H-bonding interactions were confirmed via Fermi-bands observations in FT-IR spectroscopic analysis. The mesomorphic behaviors of present SMHBLC complexes were investigated by DSC, POM and XRD measurements. The results showed that N phase is induced in most of complexes, with temperature ranges that decrease with the length of alkoxy chain, until they vanish at n = 14. All complexes examined are found to be dimorphic, exhibiting enantiotropic SmA and N phases, except the homologue **A/2B14** which is smectogenic, possessing only the SmA phase. Moreover, the temperature-dependent XRD measurements were inconsistent with the intrinsic transition of each mesophase, which is in agreement with both the DSC and POM results. Photo-physical properties of the complexes were carried by UV-spectroscopy and the investigations revealed that shift absorption bands occurred in the UV-vis spectra for the base components, confirming the complexation. Finally, the decrement of entropy changes for present complexes was attributed to the geometrical interactions difference between individuals.

Supplementary Materials: The following are available online at http://www.mdpi.com/2073-4352/10/9/801/s1, Scheme S1: Preparation of 4-(4′-pyridylazophenyl)-4′′-alkyloxybenzoates, **Bn**. Table S1: Infrared Absorption Spectra of **Bn** derivatives. Table S2: Phase transition temperatures and enthalpy of transitions of **Bn**.

Author Contributions: Data curation, H.A.A. and M.S.K.; Formal analysis, H.A.A. and M.S.K.; Funding acquisition, M.S.K.; Investigation, H.A.A. and M.S.K.; Methodology, H.A.A. and M.S.K.; Project administration, H.A.A. and M.S.K.; Resources, H.A.A.; Writing—original draft, H.A.A. and M.S.K.; Writing—review & editing, H.A.A. and M.S.K. All authors have read and agreed to the published version of the manuscript.

Funding: This research received no external funding.

Conflicts of Interest: The authors declare no conflict of interest.

References

1. Sunil, B.N.; Srinatha, M.K.; Shanker, G.; Hegde, G.; Alaasar, M.; Tschierske, C. Effective tuning of optical storage devices using photosensitive bent-core liquid crystals. *J. Mol. Liq.* **2020**, *304*, 112719. [CrossRef]
2. Hird, M. Fluorinated liquid crystals—Properties and applications. *Chem. Soc. Rev.* **2007**, *36*, 2070. [CrossRef] [PubMed]
3. Brand, H.R.; Cladis, P.E.; Pleiner, H. Symmetry and defects in the CM phase of polymeric liquid crystals. *Macromolecules* **1992**, *25*, 7223. [CrossRef]
4. Cook, A.G.; Baumeister, U.; Tschierske, C. Supramolecular dendrimers: Unusual mesophases of ionic liquid crystals derived from protonation of DAB dendrimers with facial amphiphilic carboxylic acids. *J. Mater. Chem.* **2005**, *15*, 1708. [CrossRef]
5. Alhaddad, O.; Ahmed, H.; Hagar, M. Experimental and theoretical approaches of new nematogenic chair architectures of supramolecular H-bonded liquid crystals. *Molecules* **2020**, *25*, 365. [CrossRef] [PubMed]
6. Ahmed, H.; Hagar, M.; Alhaddad, O. New chair shaped supramolecular complexes-based aryl nicotinate derivative; mesomorphic properties and DFT molecular geometry. *RSC Adv.* **2019**, *9*, 16366–16374. [CrossRef]
7. Nafee, S.S.; Ahmed, H.A.; Hagar, M. New architectures of supramolecular H-bonded liquid crystal complexes based on dipyridine derivatives. *Liq. Cryst.* **2020**, 1–14. [CrossRef]
8. Alnoman, R.B.; Ahmed, H.A.; Hagar, M.; Abu Al-Ola, K.A.; Alrefay, B.S.; Haddad, B.A.; Albalawi, R.F.; Aljuhani, R.H.; Aloqebi, L.D.; Alsenani, S.F. Induced phases of new H-bonded supramolecular liquid crystal complexes; mesomorphic and geometrical estimation. *Molecules* **2020**, *25*, 1549. [CrossRef]
9. Alnoman, R.B.; Hagar, M.; Ahmed, H.A.; Abu Al-Ola, K.A.; Naoum, M.M.; Al-Elati, F.; Abdullah Zaid, Y.; Alsharif, A.; Al-Juhani, Y.; Abulrhelh, A. Characterization of New H-Bonded Liquid Crystalline Complexes Based on Iminophenyl Nicotinate. *Crystals* **2020**, *10*, 499. [CrossRef]
10. Alhaddad, O.A.; Abu Al-Ola, K.A.; Hagar, M.; Ahmed, H.A. Chair-and V-Shaped of H-bonded supramolecular complexes of azophenyl nicotinate derivatives; mesomorphic and DFT molecular geometry aspects. *Molecules* **2020**, *25*, 1510. [CrossRef]
11. Kato, T.; Fukumasa, M.; Frechet, J.M.J. Supramolecular liquid-crystalline complexes exhibiting room-temperature mesophases and electrooptic effects. hydrogen-bonded mesogens derived from alkylpyridines and benzoic acids. *Chem. Mater.* **1995**, *7*, 368. [CrossRef]

12. Fukumasa, M.; Kato, T.; Uryu, T.; Frechet, J.M.J. The Simplest Structure of the Hydrogen-Bonded Mesogen Built from 4-Alkoxybenzoic Acid and 4-Alkylpyridine. *Chem. Lett.* **1993**, *22*, 65. [CrossRef]
13. Kato, T.; Fujishima, A.; Frechet, J.M.J. Self-Assembly of a Twin Liquid Crystalline Complex through Intermolecular Hydrogen Bondings. *Chem. Lett.* **1990**, *19*, 919. [CrossRef]
14. Kato, T.; Adachi, H.; Fujishima, A.; Frechet, J.M.J. Self-Assembly of Liquid Crystalline Complexes Having Angular Structures through Intermolecular Hydrogen Bonding. *Chem. Lett.* **1992**, *21*, 265. [CrossRef]
15. Prasad, S.K.; Nair, G.G.; Hegde, G. Dynamic Self-Assembly of the Liquid-Crystalline Smectic A Phase. *Adv. Mater.* **2005**, *17*, 2086–2091. [CrossRef]
16. Tanaka, D.; Ishiguro, H.; Shimizu, Y.; Uchida, K. Thermal and photoinduced liquid crystalline phase transitions with a rod–disc alternative change in the molecular shape. *J. Mater. Chem.* **2012**, *22*, 25065–25071. [CrossRef]
17. Alaasar, M.; Poppe, S.; Tschierske, C. Photoresponsive halogen bonded polycatenar liquid crystals. *J. Mol. Liq.* **2019**, *277*, 233–240. [CrossRef]
18. Pintre, I.C.; Serrano, J.L.; Ros, M.B.; Martínez-Perdiguero, J.; Alonso, I.; Ortega, J.; Folcia, C.L.; Etxebarria, J.; Alicante, R.; Villacampa, B. Bent-core liquid crystals in a route to efficient organic nonlinear optical materials. *J. Mater. Chem.* **2010**, *20*, 2965–2971. [CrossRef]
19. Yang, P.C.; Liu, J.H. Synthesis and characterization of novel photoisomerizable liquid crystalline polymers containing cinnamoyl groups. *J. Polym. Sci. Part A Polym. Chem.* **2008**, *46*, 1289–1304. [CrossRef]
20. Pongali Sathya Prabu, N.; Madhu Mohan, M.L.N. Characterization of a hydrogen bonded liquid crystal homologous series: Detailed FTIR studies in various mesophases. *J. Mol. Struct.* **2011**, *994*, 387–391. [CrossRef]
21. Pongali Sathya Prabu, N.; Madhu Mohan, M.L.N. Characterization of a new smectic ordering in supramolecular hydrogen bonded liquid crystals by X-ray, optical and dielectric studies. *J. Mol. Liq.* **2013**, *182*, 79. [CrossRef]
22. Pongali Sathya Prabu, N.; Vijayakumar, V.N.; Madhu Mohan, M.L.N. Thermal and dielectric studies of self-assembly systems formed by hydroquinone and alkyloxy benzoic acids. *Phys. B Condens. Matter* **2011**, *406*, 1106. [CrossRef]
23. Gopunath, A.J.; Chitravel, T.; Kavitha, C.; Pongali Sathya Prabu, N.; Madhu Mohan, M.L.N. Double Hydrogen Bonded Liquid Crystals Formed by Glutaric Acid. *Mol. Cryst. Liq. Cryst.* **2013**, *547*, 19. [CrossRef]
24. Lehn, J.M. *Supramolecular Chemistry: Concept and Perspectives*; VCH Verlagsgesellschaft: Weinheim, Germany, 1995.
25. Fouquey, C.; Lehn, J.M.; Mlevelut, A. Molecular recognition directed self-assembly of supramolecular liquid crystalline polymers from complementary chiral components. *Adv. Mater.* **1990**, *2*, 254. [CrossRef]
26. Dave, J.S.; Menon, M. Azomesogens with a heterocyclic moiety. *Bull. Mater. Sci.* **2000**, *23*, 237–238. [CrossRef]
27. Abberley, J.P.; Killah, R.; Walker, R.; Storey, J.M.; Imrie, C.T.; Salamończyk, M.; Zhu, C.; Gorecka, E.; Pociecha, D. Heliconical smectic phases formed by achiral molecules. *Nat. Commun.* **2018**, *9*, 228. [CrossRef] [PubMed]
28. Paterson, D.A.; Crawford, C.A.; Pociecha, D.; Walker, R.; Storey, J.M.; Gorecka, E.; Imrie, C.T. The role of a terminal chain in promoting the twist-bend nematic phase: The synthesis and characterisation of the 1-(4-cyanobiphenyl-4′-yl)-6-(4-alkyloxyanilinebenzylidene-4′-oxy) hexanes. *Liq. Cryst.* **2018**, *45*, 2341–2351. [CrossRef]
29. Ahmed, H.; Hagar, M.; Aljuhani, A. Mesophase behavior of new linear supramolecular hydrogen-bonding complexes. *RSC Adv.* **2018**, *8*, 34937–34946. [CrossRef]
30. Ahmed, H.; Hagar, M.; Alaasar, M.; Naoum, M. Wide nematic phases induced by hydrogen-bonding. *Liq. Cryst.* **2019**, *46*, 550–559. [CrossRef]
31. Ghosh, T.; Lehmann, M. Recent advances in heterocycle-based metal-free calamitics. *J. Mater. Chem. C* **2017**, *5*, 12308–12337. [CrossRef]
32. Zhang, X.-B.; Tang, B.-C.; Zhang, P.; Li, M.; Tian, W.-J. Synthesis and characterization of 1, 3, 4-oxadiazole derivatives containing alkoxy chains with different lengths. *J. Mol. Struct.* **2007**, *846*, 55–64. [CrossRef]
33. Chen, Y.; Yu, H.; Quan, M.; Zhang, L.; Yang, H.; Lu, Y. Photothermal effect of azopyridine compounds and their applications. *RSC Adv.* **2015**, *5*, 4675–4680. [CrossRef]
34. Garcia-Amorós, J.; Reig, M.; Cuadrado, A.; Ortega, M.; Nonell, S.; Velasco, D. A photoswitchable bis-azo derivative with a high temporal resolution. *Chem. Commun.* **2014**, *50*, 11462–11464. [CrossRef]

35. Bremer, M.; Kirsch, P.; Klasen-Memmer, M.; Tarumi, K. The TV in Your Pocket: Development of Liquid-Crystal Materials for the New Millennium. *Angew. Chem. Int. Ed.* **2013**, *52*, 8880–8896. [CrossRef] [PubMed]
36. Sacconea, M.; Kuntze, K.; Ahmed, Z.; Siiskonen, A.; Giese, M.; Priimagi, A. Ortho-fluorination of azophenols increases the mesophase stability of photoresponsive hydrogen-bonded liquid crystals. *J. Mater. Chem. C* **2018**, *6*, 9958–9996.
37. Saccone, M.; Pfletscher, M.; Kather, S.; Wölper, C.; Daniliuc, C.; Mezger, M.; Giese, M. Improving the mesomorphic behaviour of supramolecular liquid crystals by resonance-assisted hydrogen bonding. *J. Mater. Chem. C* **2019**, *7*, 8643–8648. [CrossRef]
38. Chen, Y.J.; Yu, H.F.; Zhang, L.Y.; Yang, H.; Lu, Y.F. Photoresponsive liquid crystals based on halogen bonding of azopyridines. *Chem. Commun.* **2014**, *50*, 9647. [CrossRef]
39. Pfletscher, M.; Wölper, C.; Gutmann, J.S.; Mezger, M.; Giese, M. A modular approach towards functional supramolecular aggregates—Subtle structural differences inducing liquid crystallinity. *Chem. Commun.* **2016**, *52*, 8549. [CrossRef]
40. Naoum, M.; Fahmi, A.; Alaasar, M. Supramolecular Hydrogen-Bonded Liquid Crystals Formed from 4-(4′-Pyridylazophenyl)-4″–Substituted Benzoates and 4-Alkoxybenzoic Acids. *Mol. Cryst. Liq. Cryst.* **2008**, *482*, 57–70. [CrossRef]
41. Martinez-Felipe, A.; Cook, A.G.; Abberley, J.P.; Walker, R.; Storey, J.M.; Imrie, C.T. An FT-IR spectroscopic study of the role of hydrogen bonding in the formation of liquid crystallinity for mixtures containing bipyridines and 4-pentoxybenzoic acid. *RSC Adv.* **2016**, *6*, 108164–108179. [CrossRef]
42. Cleland, W.; Kreevoy, M.M. Low-barrier hydrogen bonds and enzymic catalysis. *Science* **1994**, *264*, 1887–1890. [CrossRef] [PubMed]
43. Lizu, M.; Lutfor, M.; Surugau, N.; How, S.; Arshad, S.E. Synthesis and characterization of ethyl cellulose–based liquid crystals containing azobenzene chromophores. *Mol. Cryst. Liq. Cryst.* **2010**, *528*, 64–73. [CrossRef]
44. Martínez-Felipe, A.; Imrie, C.T. The role of hydrogen bonding in the phase behaviour of supramolecular liquid crystal dimers. *J. Mol. Struct.* **2015**, *1100*, 429–437. [CrossRef]
45. Ghanem, A.; Noel, C. FTIR investigation of two alkyl-p-terphenyl-4,4″-dicarboxylates in their crystalline, smectic and isotropic phases. *Mol. Cryst. Liq. Cryst.* **1987**, *150*, 447–472. [CrossRef]
46. Paterson, D.A.; Martínez-Felipe, A.; Jansze, S.M.; TMMarcelis, A.; MDStorey, J.; Imrie, C.T. New insights into the liquid crystal behaviour of hydrogen-bonded mixtures provided by temperature-dependent FTIR spectroscopy. *Liq. Cryst.* **2015**, *42*, 928–939. [CrossRef]
47. Walker, R.; Pociecha, D.; Abberley, J.; Martinez-Felipe, A.; Paterson, D.; Forsyth, E.; Lawrence, G.; Henderson, P.; Storey, J.; Gorecka, E.; et al. Spontaneous chirality through mixing achiral components: A twist-bend nematic phase driven by hydrogen-bonding between unlike components. *Chem. Commun.* **2018**, *54*, 3383–3386. [CrossRef]
48. Gopunatha, A.J.; Chitravela, T.; Kavithab, C.; Pongali Sathya Prabub, N.; Madhu Mohanb, M.L.N. Thermal, Optical, and Dielectric Analysis of Hydrogen-Bonded Liquid Crystals Formed by Adipic and Alkyloxy Benzoic Acids. *Mol. Cryst. Liq. Cryst.* **2014**, *592*, 63. [CrossRef]
49. Ahmed, H.; Naoum, M.; Saad, G. Mesophase behaviour of 1: 1 mixtures of 4-n-alkoxyphenylazo benzoic acids bearing terminal alkoxy groups of different chain lengths. *Liq. Cryst.* **2016**, *43*, 1259–1267. [CrossRef]
50. Saccone, M.; Spengler, M.; Pfletscher, M.; Kuntze, K.; Virkki, M.; Wölper, C.; Gehrke, R.; Jansen, G.; Metrangolo, P.; Priimagi, A.; et al. Photoresponsive Halogen-Bonded Liquid Crystals: The Role of Aromatic Fluorine Substitution. *Chem. Mater.* **2019**, *31*, 462–470. [CrossRef]
51. Dhammika Bandara, H.; Burdette, S.C. Photoisomerization in different classes of azobenzene. *Chem. Soc. Rev.* **2012**, *41*, 1809–1825. [CrossRef]
52. Zhang, X.; Feng, H.; Yan, M.; Guo, H.; Yang, F. The novel rufigallol-based liquid crystals with cholesterol units: Synthesis, mesomorphic and photophysical properties. *Liq. Cryst.* **2019**, *46*, 787–796. [CrossRef]
53. Lin, L.; Qin, W.; Cheng, B.; Guo, H.; Yang, F. The influence of multiple alkyl chains on mesomorphic and photophysical properties of diphenylacrylonitrile liquid crystals. *Liq. Cryst.* **2019**, *47*, 1–10. [CrossRef]

54. Yang, M.; Liu, Z.; Li, X.; Yuan, Y.; Zhang, H. Influence of flexible spacer length on self-organization behaviors and photophysical properties of hemiphasmidic liquid crystalline polymers containing cyanostilbene. *Eur. Polym. J.* **2020**, *123*, 109459. [CrossRef]
55. Zhang, B.Y.; Jia, Y.G.; Yao, D.S.; Dong, X.W. Preparation and properties of siloxane liquid crystalline elastomers with a mesogenic crosslinking agent. *Liq. Cryst.* **2004**, *31*, 339. [CrossRef]